

Experimental & Computational Study on Compound Delta Wing

M. Naimuddin¹, G. Chopra², G. Sharma³

^{1,2,3}Aeronautical Engineering Department
Manav Rachna International University, Faridabad

Abstract: Experimental and computational studies have been made on compound delta wing at angles of attack in the range of 0 to 15 degrees in the pitch plane. The flow field of compound delta wing is dominated by leading edge vortices. Characteristics of leading edge vortices vary with increasing angle of attack, at high angles they undergo “breakdown” or “bursting”. Experiments consisted of Surface Oil flow visualization over a Sharp Edged 47°-69° compound delta wing at free stream Reynolds Number of 3.5×10^5 based on root chord length of the wing model. Oil flow visualization reveals the Streakline pattern and this pattern have been used to infer the flow field over the surface of the wing. Subsequently computations were made using commercially available software ANSYS FLUENT. Computational domain was meshed by 3 dimensional structured grid and Reynolds Averaged Navier Stokes (RANS) based steady state computations were carried out. The results from present study indicate that the wing surface vortices dilate with increase in angle of attack and burst at high angle of attack. Moreover, the results could provide valuable inputs for vortex bursting control and design of wing structure.

1. INTRODUCTION

Compound delta wing configuration is adopted in many modern high speed fighter aircrafts like HAL Tejas (Light Combat Aircraft). Compounded delta wing configuration possibly provides better stability and maneuverability, which is essential for fighter aircrafts. Moreover, delta wing configuration also gives low supersonic drag and to further improves this thin or sharp leading edges are adopted. Due to pressure difference across the wing, flow over the lower surface moves in span-wise direction towards the upper surface and flow separates along the leading edge. This causes generation of two counter rotating leading edge vortices (LEV) over the surface of wing moving towards downstream as shown in figure 1. Vortices dominated flow-field cause's aerodynamic characteristics of the wing to become highly non-linear. Moreover, with increasing angle of attack the characteristics of LEV vary and undergo “breakdown” or “bursting”. This phenomenon causes highly unsteady aerodynamic loads on the wing might lead to buffeting. Consequently, precise information about vortex breakdown is important for designers.

Streakline pattern over the surface reveals the local flow over the wing surface. Important flow features like separation, attachment line can also be observed using wing surface streakline pattern. Therefore, a lot of work has been done to understand the flow-field over delta wings using surface flow visualization techniques. [1] Studied effect of angle of attack and Reynolds number on vertical flow behavior on 76°-40° double-delta wing. [2] Carried out oil flow visualization and stereo particle image velocimetry (SPIV) technique to understand the effect of leading edge radius on Aerodynamics of 50° sweep delta wing. [2] Reported the enlargement and spanwise outward movement of primary vortex due to vortex breakdown at 10° angle of attack and upstream movement of vortex breakdown point with increasing angle of attack.[3]

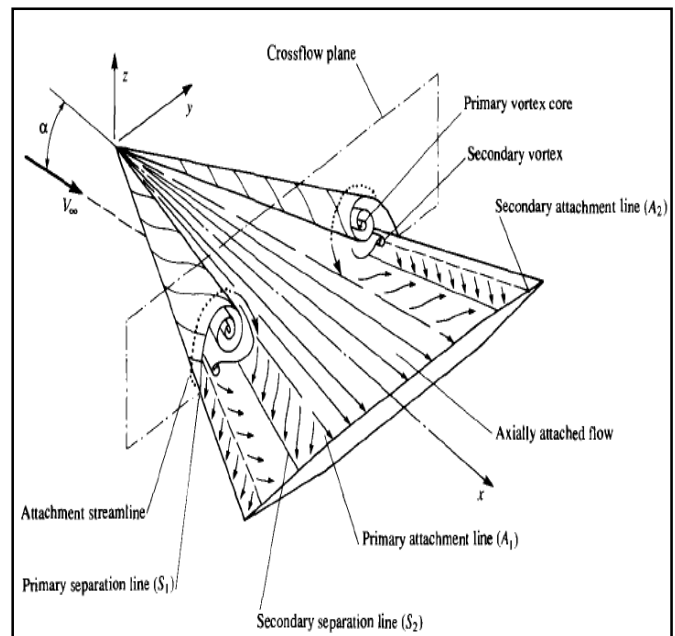


Figure 1. Schematic of flow field over delta wing [11].

Performed numerical and experimental study on 65° sweep delta wing at different angles of attack and sideslip angles. [3]

Reported asymmetric behavior of vortex breakdown. Flow over single beveled 76° - 40° double delta wing was investigated by [4]. Detailed study on vortical flow structure is reported by [5-7]. Various vortices control techniques are reported by [8-10].

Present study is focused on experimentally investigating surface flow over a sharp edged 47° - 69° compound delta wing. Experiments were carried out at 0° , 5° , 10° and 15° angles of attack and Reynolds Number of 3.5×10^5 based on root chord length of the wing model. Surface flow pattern is obtained by oil flow visualization technique. The experimental methodology and results are discussed in following sections.

2. EXPERIMENTAL METHODOLOGY

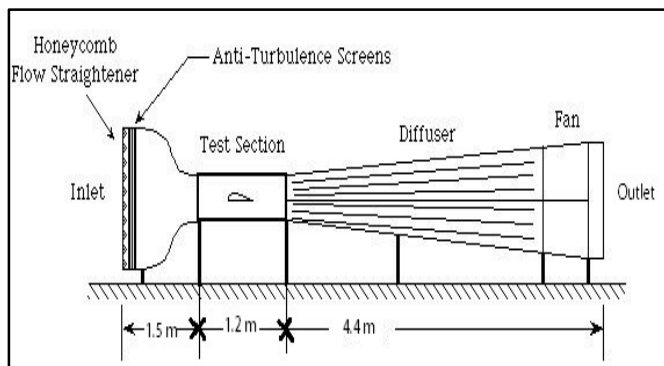


Figure 2. Schematic of Low subsonic wind tunnel setup.

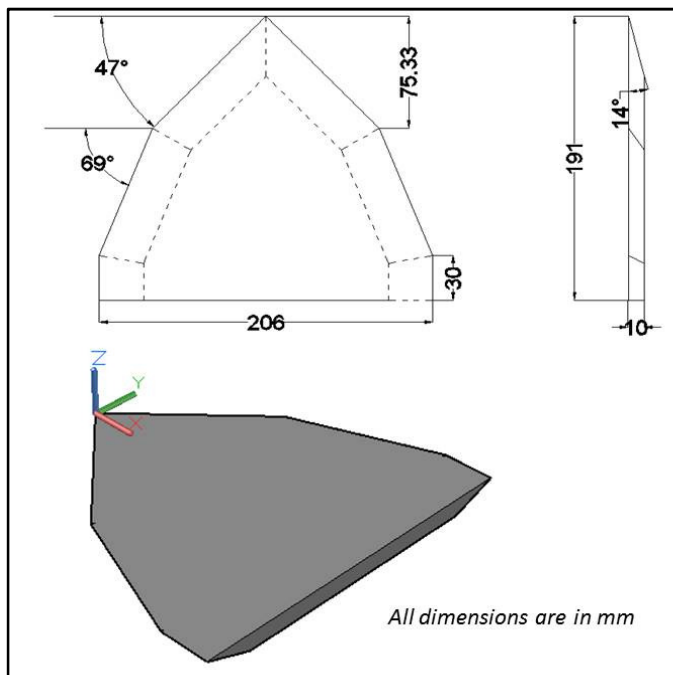


Figure 3. Geometry of compound delta wing.

All the experiments have been made using the low Subsonic Wind Tunnel at Aeronautical Engineering department of Manav Rachna International University, Faridabad. The test section has dimensions of $300\text{mm} \times 300\text{mm} \times 1200\text{mm}$ and is provided with transparent windows on top and sides walls.

Experiments were carried out at free-stream velocity of 31 m/s at Reynolds Number of 3.5×10^5 based on root chord of wing model. The studies have been made at angle of attack in the range of 0° to 15° .

The wing model is a wooden flat plate 47° - 69° compound double delta wing having sharp leading edges. The leading edge is single beveled with 14° bevel angle. The trailing edge of the wing has a plane blunt edge. The root chord of the wing model is 191 mm and the wing span is 206 mm. The wing thickness is 10 mm. The schematic drawing of the double delta wing is shown in figure 3.

The surface of the model was painted black in color to ensure the proper and distinct visibility of surface flow patterns. A mixture of titanium dioxide and oleic acid oil in the appropriate volumetric ratio of has been used for surface flow visualization studies. The mixture is painted uniformly as a thin layer on upper flat surface of the wing model.

3. COMPUTATIONAL METHODOLOGY

3D model is developed to study the flow over a compound delta wing. One half of the model is constructed for the purpose of computation as the whole object is symmetrical. Computational domain is shown in figure 4.

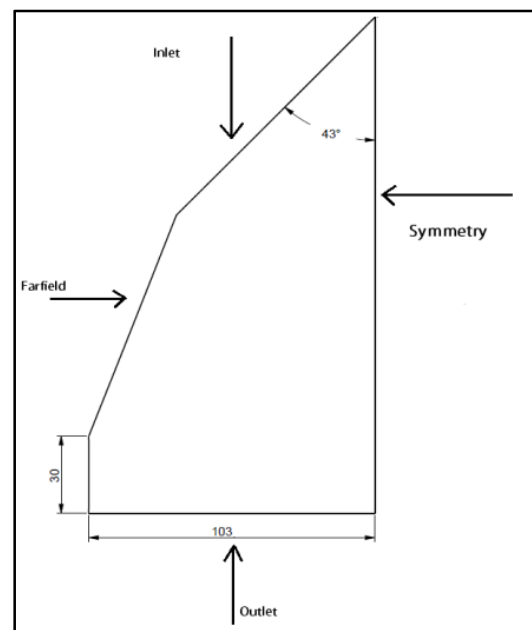


Figure 4. Computational domain.

Figure 5 shows the meshed geometry of the symmetric one half of the wing used for analysis.

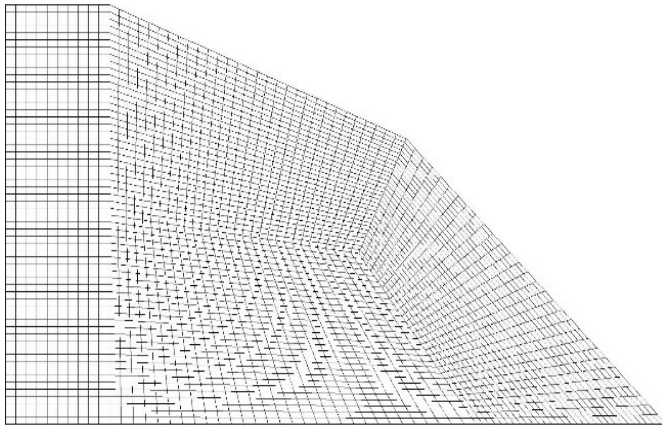


Figure 5. Surface mesh used for computation.

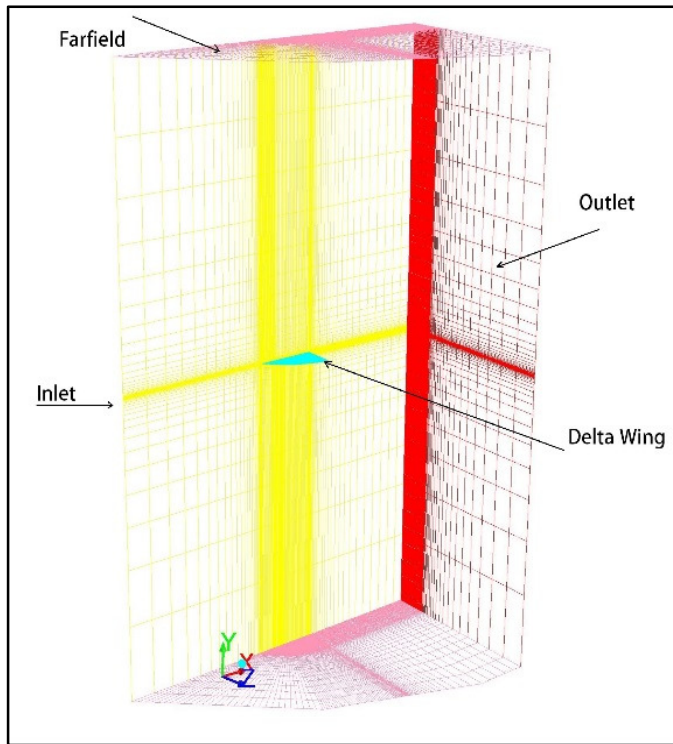


Figure 6. Meshed grid.

The conservation equations of mass, momentum and energy are solved for obtaining solution over the double delta wing.

Conservation of Mass

$$\frac{\partial \rho}{\partial t} + \Delta \cdot (\rho v) = 0$$

Conservation of Momentum

$$\rho \frac{Du}{Dt} = -\frac{\partial p}{\partial x} + \frac{\partial \tau_{xx}}{\partial x} + \frac{\partial \tau_{yx}}{\partial y} + \frac{\partial \tau_{zx}}{\partial z} + \rho f_x \quad (\text{In X-Direction})$$

Conservation of Energy

$$\begin{aligned} \rho \frac{D}{Dt} \left(e + \frac{V^2}{2} \right) = & \rho q + \frac{\partial}{\partial x} \left(k \frac{\partial T}{\partial x} \right) + \frac{\partial}{\partial y} \left(k \frac{\partial T}{\partial y} \right) + \frac{\partial}{\partial z} \left(k \frac{\partial T}{\partial z} \right) - \frac{\partial (up)}{\partial x} - \frac{\partial (vp)}{\partial y} - \frac{\partial (wp)}{\partial z} \\ & + \frac{\partial (u\tau_{xx})}{\partial x} + \frac{\partial (u\tau_{yx})}{\partial y} + \frac{\partial (u\tau_{zx})}{\partial z} + \frac{\partial (v\tau_{xy})}{\partial x} + \frac{\partial (v\tau_{yy})}{\partial y} + \frac{\partial (v\tau_{zy})}{\partial z} \\ & + \frac{\partial (w\tau_{xz})}{\partial x} + \frac{\partial (w\tau_{yz})}{\partial y} + \frac{\partial (w\tau_{zx})}{\partial z} + \rho f \cdot V \end{aligned}$$

For the accurate prediction of aerodynamic performance, the study of vortices around the wing has to be thoroughly understood. Inviscid solvers are not capable of predicting the vortex phenomena hence there lies a requirement of introduction of turbulence model therefore; Spalart Allmaras (SA) model is used. SA is a one equation turbulence model which requires less computation time when compared to other turbulence models and is very suitable for predicting aerodynamic flows. The equations can be described as:

$$\begin{aligned} \frac{\partial}{\partial t} (\rho \tilde{v}) + \frac{\partial}{\partial x_i} (\rho \tilde{v} u_i) & = G_v \\ & + \frac{1}{\sigma_{\tilde{v}}} \left[\frac{\partial}{\partial x_j} \left\{ (\mu + \rho \tilde{v}) \frac{\partial \tilde{v}}{\partial x_j} \right\} + C_{b2} \rho \left(\frac{\partial \tilde{v}}{\partial x_j} \right)^2 \right] \\ & - Y_v + S_{\tilde{v}} \end{aligned}$$

\tilde{v} is transport variable (analogous to the turbulent kinematic viscosity except near-wall (viscous-affected) region). G_v is production of turbulent viscosity, Y_v is the destruction of turbulent viscosity that occurs in the near-wall region due to wall blocking and viscous damping, $\sigma_{\tilde{v}}$ and C_{b2} are constants and ν is the molecular kinematic viscosity, $S_{\tilde{v}}$ is user-defined source term.

Turbulent viscosity, μ_t , is computed from:

$$\mu_t = \rho \tilde{v} f_{v1}$$

Where f_{v1} is viscous damping function and it is given by:

$$f_{v1} = \frac{\chi^3}{\chi^3 + C_{v1}^3}$$

$$\chi \equiv \frac{\tilde{v}}{\nu}$$

G_v is modelled as:

$$G_v = C_{b1} \rho \tilde{S} \tilde{v}$$

$$\tilde{S} \equiv S + \frac{\tilde{v}}{\kappa^2 d^2} f_{v2}$$

$$f_{v2} = 1 - \frac{\chi}{1 + \chi f_{v1}}$$

C_{b1} and κ are constants, d is the distance from the wall, and S is a scalar measure of the deformation tensor.

The destruction term:

$$Y_v = C_{w1} \rho f_w \left(\frac{\tilde{v}}{d} \right)^2$$

$$f_w = g \left[\frac{1 + C_{w3}^6}{g^6 + C_{w3}^6} \right]^{1/6}$$

$$g = r + C_{w2}(r^6 - r)$$

$$r \equiv \frac{\tilde{v}}{S \kappa^2 d^2}$$

C_{w1} , C_{w2} and C_{w3} are constants. Modifications done to include the effects of mean strain on S will also affect the value of \tilde{S} used to compute r .

$$C_{b1} = 0.1355, C_{b2} = 0.622, \sigma_{\tilde{v}} = \frac{2}{3}, C_{v1} = 7.1, C_{w1} = \frac{C_{b1}}{\kappa^2} + \frac{(1 + C_{b2})}{\sigma_{\tilde{v}}}, C_{w2} = 0.3, C_{w3} = 2, \kappa = 0.4187$$

Modified turbulent kinematic viscosity \tilde{v} is set to zero.

The meshing of the model has been done using GAMBIT software. As the structure of the wing is symmetrical so half of the body is used in the domain to save computation time. A stationary no slip boundary condition is imposed on the walls of the wing. Schematic of the discretized domain is shown in figure 5. Grid independence tests have been performed on the model. A total of 612400 cells have been used in the model. Figure 6 shows the meshed geometry along with whole domain of the flow. Coupled scheme has been used for the solution purpose. Y^+ and other Turbulence parameters have been maintained for all the computations at different angle of attack.

4. RESULTS AND DISCUSSIONS

A typical surface flow pattern obtained by oil flow visualization technique on the surface of wing at 0° angle of attack is shown in figure 7. Most flow features like axially attached flow lines, separation line and attachment line are clearly visible on the surface flow pattern obtained by oil flow visualization technique. At 0° angle of attack vortex appears to emerge from the kink and move downstream along with wing tip. Near the root of the wing flow is observed to be attached and move in axial direction.

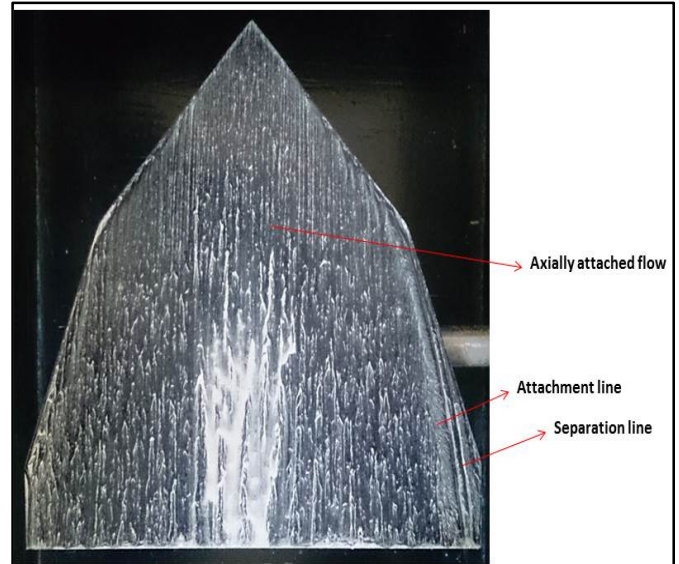


Figure 7. Surface flow pattern at 0° angle of attack.

Moreover, as the angle of attack is increased to 5° the flow field changes significantly, as shown in figure 8. The point of emergence of vortex has moved up from the kink to the apex. The vortex appears to enlarge as it moves downstream. The attachment line moves inboard, this may be due to vortex enlargement.

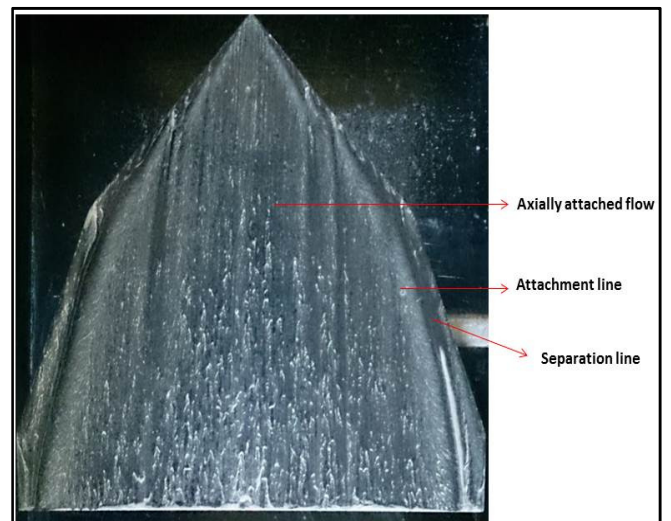


Figure 8. Surface flow pattern at 5° angle of attack.

Wing surface streakline pattern obtained from computations is able to capture the flow phenomenon with appreciable degree of accuracy. The vital flow features like attachment line, separation line are comprehensible as shown in figures 9, 10. Therefore, Computational and experimental surface flow patterns are in good agreement with each other.

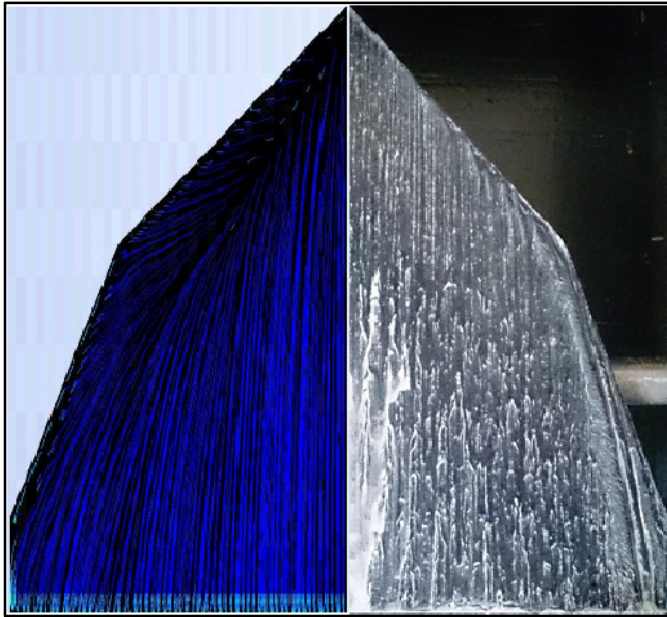


Figure 9. Computational and Experimental surface flow pattern at 0° angle of attack.

As the angle of attack is further increased to 10°, the flow features become clearly visible and significant on the surface flow pattern as shown in figure 11. This may be because of increasing strength and size of vortex. The attachment line moves further inwards. Vortex appears to emerge from apex of the wing and move downstream. At the root flow remains attached and moves in axial direction.

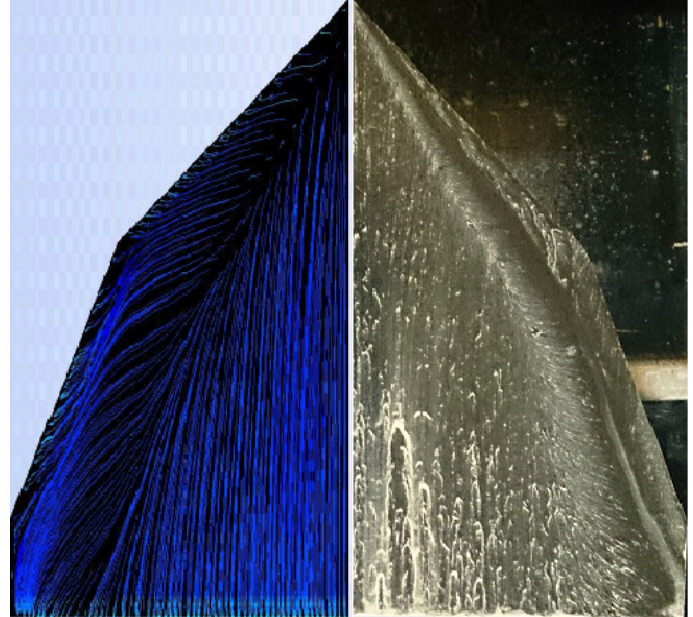


Figure 11. Computational and Experimental surface flow pattern at 10° angle of attack.

Figure 12 shows surface flow pattern at 15° angle of attack. The flow features are easily discernable; this may be because of increase in strength and size of vortex. Furthermore, the vortex gets distorted at this angle of attack, this can be observed from outward movement of flow near the trailing edge of the wing. Flow-field indicates towards the vortex breakdown or bursting phenomenon, this is accompanied by unsteady and asymmetric behavior.

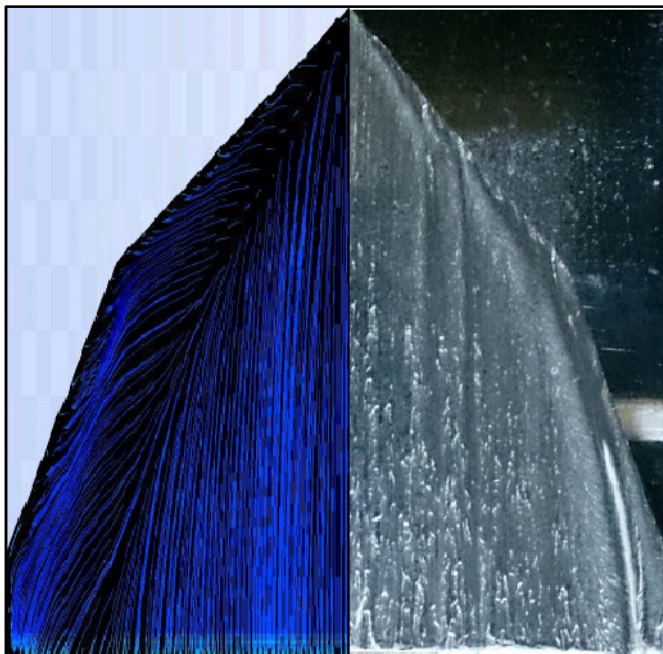


Figure 10. Computational and Experimental surface flow pattern at 5° angle of attack.

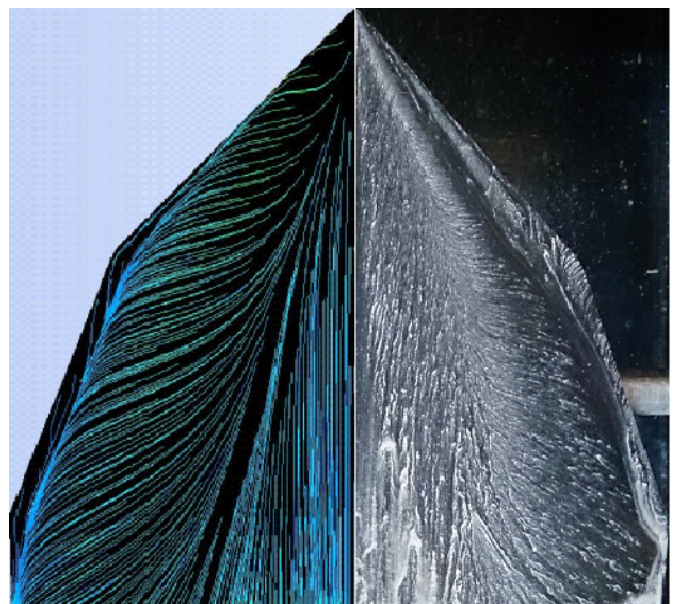


Figure 12. Computational and Experimental surface flow pattern at 15° angle of attack.

5. CONCLUSION

A preliminary investigation is presented of flow over 47°-69° compound delta wing at angles of attack in the range of 0° to 15°.

Strength and size of the vortex increase with the angle of attack. Moreover, the attachment line moves inward as angle of attack is increased. Vortex breakdown or bursting was observed at 15° angle of attack.

Computational and experimental wing surface flow pattern are in good agreement and provide comprehensible surface flow pattern. Vortical flow features like separation, attachment lines and phenomenon like vortex bursting are clearly noticeable for investigation

This investigation provides us a good platform to study more about the flow physics and various vortex bursting control techniques. The present computational model can be used for testing the effectiveness and understand the working of these techniques.

REFERENCES

- [1] Verhaagen N.G. and Jobe C.E., "Wind tunnel study on a 65-deg Delta Wing at side slip", *JOURNAL OF AIRCRAFT*, Vol. 40, No. 2, 2003.
- [2] Verhaagen N.G., "Effects of Leading-Edge Radius on Aerodynamic Characteristics of 50° Delta Wings", 48th AIAA Aerospace Sciences Meeting Including the New Horizons Forum and Aerospace Exposition, 2010, Florida.
- [3] Nath. B., Das. S. And Prasad. J.K., "Investigation of flow field over blunted Delta wing", 3TH International Symposium on Applied Aerodynamics and Design of Aerospace Vehicles, SAROD-2007, Thiruvananthapuram
- [4] Saha. S., Majumdar. B., "Modeling and Simulation on Double Delta Wing", *Journal of Advanced Computer Research*, Vol. 3, No. 1, Issue 8, 2013.
- [5] Ahmad. Z. Al-Garni, Farooq Saeed, Abdullah M.Al-Garni, Ayman Abdullah, Ayman Kassem, "Experimental and Numerical Investigation of 65-deg delta and 65/40 – deg double delta wings", AIAA paper 2006-0063.
- [6] Honkan. A., and Andreopoulos. J., "Instantaneous three dimensional vorticity measurements in vertical flow over a delta wing", *AIAA Journal*, Vol.35, No.10, 1997.
- [7] Yanitepe. B., and Rockwell. D., "Flow structure on a Delta wing of low sweep angle", *AIAA Journal*, Vol.42, No.3, March. 2004, pp. 513-523.
- [8] Gutmark Ephraim J and Guillot Stephen A., "Control of vortex breakdown over highly swept wings", *AIAA Journal*, Vol.43, No.5, Sept. 2005, pp.2065-2069.
- [9] Gursul. I., Wang. Z. and Vardaki E., "Review of Flow Control Mechanisms of Leading-Edge Vortices", AIAA paper 2006-3508.
- [10] J.J. Wang, Q.S. Li, J.Y. Liu, "Effect of vectored trailing jet on delta wing vortex breakdown", *Experiments in fluids* 34(2003) 651-654.
- [11] Anderson, J. D. Jr., "Fundamentals of Aerodynamics, McGraw-Hill Inc.", USA, pp. 356-361. 1991.